

COVER PAGE

Document downloaded by @DAEL

Tue Nov 10 11:56:03 2026
For personal use

When automatic English translation is provided, only the original document is authentic.
The EAA cannot be held responsible of any translation error

Bibliographical reference

Application of Statistical Weather Data From the Numerical Weather Prediction Model COSMO-2 for Noise Mapping Purposes, J.M. Wunderli and M.W. Rotach, Acta Acustica **vol. 97** (Number 3), 2011, pp. 403-415

DOI
https://doi.org/10.3813/AAA.918421

Acta Acustica united with Acustica
Vol. 97 (2011) 403 – 415

DOI 10.3813/AAA.918421

Application of Statistical Weather Data From the Numerical Weather Prediction Model COSMO-2 for Noise Mapping Purposes

J. M. Wunderli[1)], M. W. Rotach[2)*]

[1)] Empa, Swiss Federal Laboratories, for Materials Science and Technology, 8600 Duebendorf, Switzerland. jean-marc.wunderli@empa.ch

[2)] Federal Office for Meteorology and Climatology, Federal Department of Home Affairs FDHA, 8044 Zurich, Switzerland

Summary

sonRAIL is a new Swiss simulation model for railway noise. Its propagation model is applying a ray tracing approach to take meteorological influences on sound propagation into account. The ray tracing algorithm is designed to allow for arbitrary sound speed profiles, which additionally can vary along the propagation path, for example as a consequence of changing surface properties. In order to do noise mapping for long-term averages, weather statistics for entire Switzerland were derived on the basis of model data of COSMO-2, the most recent version of the operational numerical weather prediction model of the Swiss Federal Office of Meteorology and Climatology, *MeteoSwiss*, with a grid resolution of 2.2 x 2.2 km^2. Especially in regions with complex topography, as it is the case in Switzerland, this high spatial resolution is a major advantage. Additionally, a profile generator was devised, which allows to calculate vertical profiles of wind speed, temperature and humidity based on input data describing the general meteorological conditions and the local surface properties. Based on this profile generator a classification scheme for meteorological conditions was developed and a set of standard profile functions for wind speed and temperature is given for each class. The validation of the profile generator in comparison with profiles directly taken from COSMO-2 showed good agreement in general, but with a tendency to overestimate temperature gradients under highly stable conditions. A comparison of the probability of occurrence of the meteorological classes derived from COSMO-2 with observation data of conventional stations also yielded a high compliance. However nighttime situations with hardly any wind were underpredicted by COSMO-2. These findings confirm the fact that meteorological modeling is generally most difficult for low wind stable conditions. Yet the advantage of having meteorological statistics available in a small spatial resolution clearly outweighs this restraint.

PACS no. 43.50.+y

1. Introduction

Modern calculation models for noise assessment aim at representing sound propagation effects more accurately and closer to the physical processes than traditional tools allowed for. One of the areas of interest are meteorological effects as they have a major influence on sound exposure for distances greater than about 300 m. Most important are the vertical gradients of temperature and wind as they lead to sound propagation along curved paths. Under favorable propagation conditions shielding effects can be reduced or even canceled out while under unfavorable conditions acoustical shadow zones can evolve. Second order meteorological effects include, on the one hand, the depence of air absorption on actual values of temperature and relative humidity and, on the other hand, the influence of turbulence on the phase relation between different sound waves as well as the scattering of sound.

A common approach to represent these curved sound rays, which is implemented for example in the Harmonoise engineering model [1] or in Nord2000 [2], is to use circular sound rays. The major advantage of this approach is that the solution that leads from source to receiver can be found analytically and hence very efficiently in terms of calculation demand. However, an important constraint of this solution is that circles only develop for sound speed gradients constant with height. This precondition is hardly ever fulfilled in an environmental context. Typically gradients of wind speed and potential temperature tend to decrease with height and get negligibly small after some tens of meters. Therefore the assumption of circular sound rays yields misleading results for greater propagation distances as the rays reach heights above ground

Received 30 July 2010,
accepted 15 February 2011.

* present affiliation: University of Innsbruck, Institute for Meteorology and Geophysics, Innsbruck, Austria

Document downloaded by @DAEL, 2026-11-10 11:56:05 - personal use only

where in reality no downbending of rays takes place and therefore no favorable conditions can be found anymore.

Therefore it was decided for *sonRAIL*, the new Swiss railway noise model [3], to use a more general approach based on ray tracing [4] which allows to consider arbitrary sound speed profiles. In acoustical shadow zones where no sound rays arrive at the receiver an empirical extension is used according to Hofmann [5] that is based on geometrical properties of the ray that comes closest to the receiver. The sound speed profiles for *sonRAIL* can either be derived from measured or calculated profiles of wind and temperature and they can vary along the propagation path, for example as a consequence of changing surface properties.

The ray tracing approach implemented in *sonRAIL* has been validated amongst others in comparison with a Finite-Differences-in-the-Time-Domain-model [6], [7]. The comparison showed good agreement for downwind as well as upwind conditions (see [3], chapter 7). The validation calculations have been performed for distinct meteorological situations based on temperature and wind profiles over grassland taken from the literature (see for example [8]). Here, we address the problem of how to obtain such profiles for practical applications.

For distinct conditions meteorological theory allows to predict the necessary profile functions that can, for example, be used for comparisons with single measurement results [9]. In order to calculate long-term averages statistics of the underlying meteorological parameters have to be available. And for noise mapping, which is generally based on long term averages, it is additionally necessary to have such meteorological statistics at hand for the entire area of calculation. Especially in regions with a complex topography these statistics have to be available in high spatial resolution as mainly wind fields can exhibit major changes within only a few hundred meters distance (see for example [10]). Generally, data from conventional meteorological stations are distributed in the range of several tens of kilometers distance at best (recommended are 'every 10 km' in mountainous terrain what can never be reached in practice due to the enormous costs). Given the spatial density of meteorological observations and the challenges for spatial interpolation in complex terrain (e.g., [11]) an alternative is to use analysis fields from numerical weather prediction (NWP) modeling. These analysis fields are being produced at the beginning of every NWP run (daily or even more frequently) and as they take into account latest observations they may therefore be viewed as a daily available, physically based interpolation scheme.

In cooperation with the Federal Office of Meteorology and Climatology *MeteoSwiss* it was therefore decided to rely on model data of COSMO-2, instead of measurements. COSMO-2 is the most recent version of the operational numerical weather prediction model COSMO with a grid resolution of $2.2 \times 2.2\,\mathrm{km}^2$ and 60 model surfaces, i.e., vertical levels at which values are given. NWP models are based on solving the conservation equations for momentum, energy and mass (e.g., [12]) and thus produce physically based 3-D meteorological fields which are, of course, limited by simplifying assumptions and grid resolution.

In this publication a methodology to derive local weather statistics on this basis is presented and prospects as well as restraints of such an approach are discussed. The methodology is strongly connected to a profile generator described in section 3 that allows to generate wind speed, temperature and humidity profiles to be used as input for sound propagation models. Section 4 yields a statistical analysis procedure with a classification scheme that has been derived based on experiences with the profile generator. In section 5 profiles of wind speed and temperature of COSMO-2 are compared with the corresponding results of the profile generator and wind distribution data of COSMO-2 is validated in comparison with measurements.

2. The numerical weather prediction model COSMO-2

COSMO is a numerical weather prediction model based on the physical laws describing the atmospheric and surface processes (e.g., conservation of energy and mass within the media – either air or soil – and transfer of energy and mass between the media), suitable initial and boundary conditions, and a numerical method to solve the resulting system of complex mathematical equations. It is developed within an international collaboration. The seven national weather services of Germany, Greece, Italy, Poland, Romania, Russia, and Switzerland closely collaborate within the Consortium for Small-Scale Modeling (COSMO).

With COSMO it is possible to generate regional and local forecasts in complex topography. A detailed image of the future state of the atmosphere is computed, from the low stratosphere to the surface, including the evolution of the snow cover, the lake temperatures and the soil characteristics. Forecasts are available up to three days in advance on a domain covering central and western Europe (so called COSMO-7), and more detailed up to 24 hours in advance on a domain including the Alpine arc (so called COSMO-2).

Forecast quality is largely dependent on producing suitable initial conditions (so-called assimilation). Thus COSMO invests considerable resources in producing them as accurately as possible (see for example [13]) by bringing the model initial fields closely to observations from radar, radio soundings, surface networks and aircraft observations. In the context of the present project, COSMO-derived initial fields are employed as the optimally model-interpolated observations and provide meteorological conditions at a high spatial resolution for the entire area of interest, i.e., whole Switzerland. The COSMO models are regularly validated using the operational network of surface meteorological stations (*SwissMetNet*) and radio soundings (e.g., [14], [15], [16]).

COSMO-2 is only operational since the end of February 2008. As a basis for statistical analysis it was therefore de-

Document downloaded by @DAEL, 2026-11-10 11:56:05 - personal use only

cided to use the assimilation data, i.e., the reproduction of the actual situation, of an entire year, from March 1st 2008 until February 28, 2009. A time series of only one year is exceptionally short for meteorological statistics. However, the benefit of a high spatial resolution was judged to be more important than the requirement of long climatological series. For each hour within this period the following data was obtained in a horizontal grid of 190×130 points:

- long-wave and short-wave radiation balance,
- global and long-wave incoming radiation,
- temperature at a height of 2 m,
- temperature, relative humidity, wind speed and wind direction at a height of approximately 10 m (i.e., the lowest model surface),
- temperature, wind speed and -direction at heights of approximately 33 m, 65 m, 108 m and 160 m (model surfaces 2 to 5)

Additionally for each grid point the geographical location, the distribution of land and water, the surface roughness, z_0, split up into two contributions from the local surface properties and from sub-grid scale topography, the surface type, the height above sea level as well as the exact heights of the model surfaces are given.

3. The profile generator

The data available from COSMO-2 as presented in the previous section provide an adequate basis for meteorological statistics. However, as the conditions are only defined at a few distinct heights it is not sufficient to directly derive vertical profiles of wind, temperature and potentially also humidity, which are needed as input for sound propagation calculations. Especially close to the ground there is not enough data to reproduce complete profiles. Furthermore, COSMO profiles are determined for an average ground roughness over a single grid (e.g. [17]), i.e. an area of more than 4 kilometers squared. For the demands of acoustical modeling this classification of surface roughness is generally too coarse.

It was therefore decided to develop a tool, which allows for the calculation of wind speed, temperature and humidity profiles based on a description of the general meteorological conditions and the local surface properties. As a precondition it was defined that it should be possible to collect the necessary input data also based on conventional meteorological stations in order to expand the range of application, for example for validation measurements in the field.

The method is based on common knowledge about meteorological theory, i.e. the Monin-Obukhov Similarity Theory (see for example [8], [18]). It employs a so-called 'meteorological preprocessor' according to Hanna and Chang [19] to assess the corresponding similarity parameters and uses several extensions and adoptions for the specific demands of acoustical modeling. The model aims at reproducing profile functions for the first 100 m of height above ground, as this is typically the range that has to be taken into account when dealing with meteorological effects on sound propagation of sources located close to the ground. The connection to the data given by COSMO-2 is performed by using a classification scheme as described in section 4.

The various steps of the resulting profile generator are briefly outlined in the following. For detailed information it is referred to the documentation of the *sonRAIL* project [3].

3.1. Input parameters

The profile generator needs three types of input data. The location is described by the average height of roughness elements h_r, a factor a for the energy flux into the ground and a factor α, which describes the availability of moisture in the ground. (Estimates for a and α can be taken from [20]). The meteorological situation is on the one hand defined by the the net radiation balance at the surface Q_*, that can be calculated according to [21], and by the percentage of cloud cover. On the other hand data of wind speed, temperature and humidity at a single height within the surface layer, i.e. the lowest approximately 10% of the Planetary Boundary layer, are needed.

3.2. Calculation of the surface radiation balance

As a first step the surface radiation balance is calculated according to an approach based on the Priestley-Taylor parametrization to derive the sensible heat flux Q_h. However, as a modification with respect to the approach in [19] the empirical factor β', that represents a correction for advection, is set to 5 W/m^2 (rather than 20 W/m^2 in [19]). This modification reflects the results of some tuning in order to obtain better result in the present area of application (i.e., Switzerland).

$$Q_h = \left[\frac{(1-\alpha)+S}{1+S}\right]\cdot Q_*\cdot(1-a) - \alpha\cdot\beta' \qquad (1)$$

with α: Factor describing the availability of moisture in the ground, S: Linear approximation, valid from −5 °C to 35 °C according to equation (2), a: Factor describing the energy flux into the ground, Q_*: Net radiation balance, including long- and shortwave components [W/m^2], β': Correction term for advection = 5 W/m^2.

$$S = \frac{c_p}{L_e\cdot(\mathrm{d}q_s/\mathrm{d}T)} \approx 0.21 + \frac{1.8}{40\cdot(35 - T[^\circ\mathrm{C}])}, \qquad (2)$$

with: c_p: specific heat of dry air at constant pressure = 1005 J/kg/K, L_e: Evaporation energy of water = $2.5\cdot 10^6$ J/kg, $(\mathrm{d}q_s/\mathrm{d}T)$: Gradient of the saturation of humidity in air (Clausius-Clapeyron-Equation).

3.3. Estimation of the friction velocity u_*

The friction velocity u_* is a characteristic parameter for the description of the wind speed profile and responds to the surface character. During daytime, when $Q_h > 0$, an estimate of the u_* is determined according to

$$u_* = \frac{k\cdot v_m}{\ln\left[\frac{z_m - 0.5h_r}{z_0}\right]}\left[1 + d_1\cdot\ln(1 + d_2\cdot d_3)\right], \qquad (3)$$

Document downloaded by @DAEL, 2026-11-10 11:56:05 - personal use only

with k: von Karman constant ≈ 0.4, v_m: horizontal component of the wind speed at height z_m [m/s], h_r: height of roughness elements [m], z_0: roughness length [m] $\approx 0.1 h_r$, d_1: if $z_0/(z_m - 0.5h_r) \leq 0.01$: $d_1 = 0.128 + 0.005 \cdot \ln[z_0/(z_m - d)]$, else $d_1 = 0.107$, d_2: $1.95 + 32.6[z_0/(z_m - 0.5h_r)]^{0.45}$, d_3:

$$\frac{Q_h}{\rho \cdot c_p} \frac{k \cdot g \cdot (z_m - 0.5h_r)}{T_m} \left[\frac{\ln\left[(z_m - 0.5h_r)/z_0\right]}{k \cdot v_m} \right]^3,$$

g: gravity constant ≈ 9.81 m/s^2, T_m: temperature at height z_m [K].

At nighttime, when $Q_h \leq 0$, an estimate of u_* is calculated according to

$$u_* = \frac{k \cdot v_m}{2 \cdot \ln\left[\frac{z_m - 0.5h_r}{z_0}\right]} \cdot \left[1 + \sqrt{1 - 4\left(\frac{4.7 \cdot g \cdot z_m \cdot \Theta_* \cdot \ln[(z_m - 0.5h_r/z_0)]}{k \cdot T_m \cdot {v_m}^2}\right)}\right]. \quad (4)$$

The turbulent temperature scale Θ_* is estimated on the basis of equation (5).

$$\Theta_* = \min\left[0.09(1 - 0.5 \cdot N^2), \frac{k \cdot T_m \cdot v_m^2}{18.8 \cdot g \cdot z_m \cdot \ln[(z_m - 0.5h_r)/z_0]}\right] \quad (5)$$

with N: The percentage of cloud cover.

As an additional specification the product of u_* and Θ_* is limited to 0.05 Km/s. In case of exceedance Θ_* is reduced in small steps until the criterion is fulfilled.

Equations (3) and (4) have been derived on the basis of the profile functions of Businger et al. [22]. It is assumed that the natural logarithm of the expression $(z_m - 0.5h_r)/z_0$ yields a positive value. This is only guaranteed if $\frac{z_m}{h_r} > 0.6$.

3.4. Calculation of derived quantities

Based on the friction velocity u_* the similarity parameters for temperature, Θ_*, and humidity, q_*, can be determined (see [23] and [24]). (Note: The estimate of Θ_* according to equation (5) is replaced.)

$$\Theta_* = \frac{-Q_h}{\rho \cdot c_p \cdot u_*}, \quad (6)$$

$$q_* = \frac{-Q_e}{\rho \cdot L_e \cdot u_*}, \quad (7)$$

with ρ: Density of air ≈ 1.225 kg/m^3 (at sea level), Q_e: Latent heat flux (by means of transport of humitidy) [W/m^2], $Q_e = Q_* - Q_g - Q_h = Q_*(1 - a) - Q_h$, with Q_g as the heat flux into the ground [W/m^2]

Additionally the Obukhov length L and the mixing depth h are calculated. The Obukhov length L characterizes the atmospheric stability. L is a positive number under stable conditions and negative in an atmosphere with unstable stratification. In a neutrally buoyant boundary layer L goes to $\pm\infty$. The mixing height h corresponds to the height up to which turbulence prevails. It is also often referred to as boundary layer height.

$$L = \frac{\overline{\Theta} \cdot {u_*}^2}{k \cdot g \cdot \Theta_*} = -\frac{{u_*}^3 \cdot \overline{\Theta} \cdot \rho \cdot c_p}{k \cdot g \cdot Q_h}, \quad (8)$$

with $\overline{\Theta}$: Average potential temperature [K].

$$h = \frac{L}{3.8}\left[-1 + \sqrt{\frac{1 + 2.28 \cdot u_*}{f \cdot L}}\right] \quad (9)$$

with f: Coriolis parameter, for mid-latitudes $\approx 10^{-4}$ s^{-1}

3.5. Calculation of vertical profiles using a LinLog-approach

As mentioned before, vertical profiles of wind speed, temperature and humidity can be derived by using dimensionless profile relations [9]. As an alternative a two- or three-parameter description of wind and temperature profiles based on a linear and a logarithmic contribution, as proposed by Heimann [25], can be used:

$$u(z) = a_{u,log} \cdot \ln\left[\frac{z - d + z_0}{z_0}\right] + a_{u,lin} \cdot (z - d) \quad (10)$$

$$T(z) = a_{0,T} + a_{T,log} \cdot \ln\left[\frac{z - d + z_0}{z_0}\right] + a_{T,lin} \cdot (z - d) \quad (11)$$

The determination of the free parameters of these LinLog-profiles from the Monin-Obukhov scaling parameters is described in [26],

$$a_{u,log} = \frac{u_*}{k}, \quad (12)$$

$$a_{u,lin} = \frac{u_*}{k}\frac{1.0}{L} \quad \text{(unstable)}, \qquad a_{u,lin} = \frac{u_*}{k}\frac{4.7}{L} \quad \text{(stable)}, \quad (13)$$

$$a_{T,log} = 0.74\frac{\Theta_*}{k}, \quad (14)$$

$$a_{T,lin} = \frac{\Theta_*}{k}\frac{0.74}{L} + \gamma_d \quad \text{(unstable)}, \qquad a_{T,lin} = \frac{\Theta_*}{k}\frac{4.7}{L} + \gamma_d \quad \text{(stable)}, \quad (15)$$

with
γ_d: Dry adiabatic temperature gradient $= -0.0098$ K/m.

The LinLog-profiles for the absolute humidity are calculated using the same approach as for temperature.

3.6. Optimization of the similarity parameters

Within the profile generator the wind speed is known at two heights. On the one hand at the height at which the input parameters were given and on the other hand directly at the surface, where it has to be zero by definition. By applying the derived profile functions it is checked whether the wind speed can be reproduced accurately at these two heights. If needed the matching is improved by adjusting the estimation of the friction velocity u_* from point 3.3. Consequently also the other parameters of the similarity theory according to point 3.4 are adjusted.

Document downloaded by @DAEL, 2026-11-10 11:56:05 - personal use only

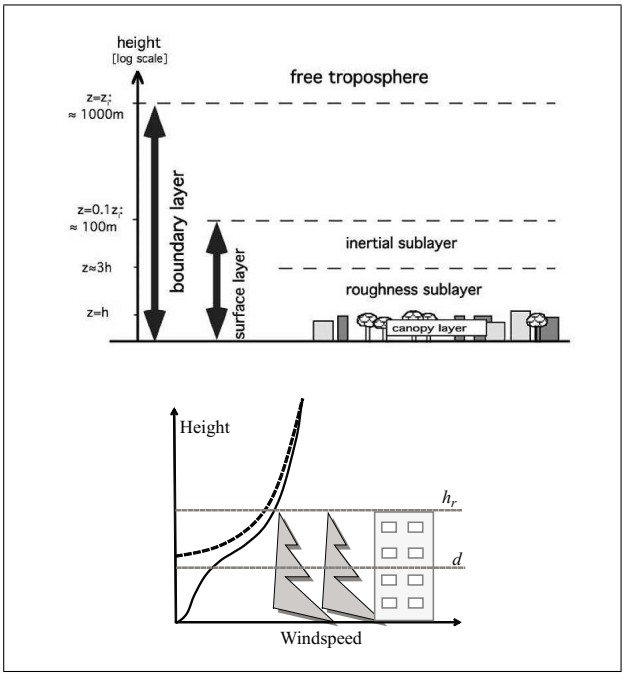


Figure 1. Top: Introduction of the roughness sublayer in the vicinity of trees and buildings. Bottom: Comparison of wind speed profiles with only a displacement of the profile functions (dashed line) with real wind speed profiles (continuous line) (Adapted from [28]).

3.7. Displacement length d and the introduction of a roughness sublayer for wind profiles

Strictly speaking, the Monin-Obukhov Similarity Theory is only valid for heights much larger than the roughness length ($z \gg z_0$). Therefore a displacement length d, set to five times z_0, is introduced. This is at the lower limit of the 'rule-of the-thumb estimates in [27] for low density canopies. The vertical profiles only start at this height. At lower heights the gradients of wind speed, potential temperature and absolute humidity are assumed to be zero (for the validity of this assumption, see e.g. [28]).

While for small z_0 this Roughness Sublayer is negligibly shallow, it can extend over several tens of meters over vegetation or urban areas (i.e., large z_0). In the presence of such greater roughness elements this approach leads to a sharp transition with very steep gradients above d. Therefore a modification of the wind profiles according to [28] has been introduced for heights $z < h_r$ to also be able to reproduce wind profiles in the canopy layer. Figure 1 shows the stratification of the atmosphere close to the ground and demonstrates the resulting wind speed profiles with and without applying the modification for the roughness sublayer.

$$v(z) = v(h_r)\cdot\exp\left[-2\left(1-\frac{z}{h_r}\right)\right] \qquad (16)$$

At a height $z = 0$ m equation (16) yields a wind speed slightly greater than zero. As the wind speed should be zero at this height per definition, the resulting profiles are corrected by fading them out linearly, starting from 0.5 m above the surface.

3.8. Extrapolation of the LinLog-profiles for greater heights

With LinLog-profiles the characteristics of the dimensionless profile relations can be reproduced very accurately with the advantage of only requiring very few parameters for their definition. Therefore they are very appropriate for classification and the description of profiles in general. It has to be borne in mind though, that the parametrization for the LinLog-profiles is only valid up to a height corresponding to the Obukhov length L. An extrapolation to greater heights can lead to contradictory devolutions of the profiles. As the Obukhov length can significantly drop below 100 m under very stable or very unstable conditions the LinLog-profiles are modified in the profile generator. It is assumed that the wind speed gradient as well as the gradient of potential temperature converge to zero at greater heights. The gradients resulting from the LinLog parameters are faded out above a starting height z_s with a decay rate p. The resulting profiles P for wind speed, temperature and humidity are calculated according to equation (17). The values for z_s and p, which are given in equation (17), have been derived in comparison with the original profiles based on meteorological theory,

$$\begin{aligned} P(z > z_s + d) = {} & a_0 + a_{lin}\cdot z_s + a_{log}\ln\left(\frac{z_s+z_0}{z_0}\right) \\ & + \left(a_{lin} + a_{log}\frac{1}{z_s+z_0}\right) \\ & \cdot\left(-p\cdot L\right)\cdot\left(1-\mathrm{e}^{-\frac{z-(z_s+d)}{pL}}\right) \end{aligned} \qquad (17)$$

with $z_s := s\cdot\min[L, h]$, with $s = 0.5$ for stable stratifications and $s = 0.7$ for neutral or unstable stratifications. p: 0.7 for stable stratifications and 2.0 for neutral or unstable stratifications.

3.9. Modification for small wind speeds

Similarity theory is based on the assumption of a turbulent boundary layer subject to considerable turbulent mixing. Under very stable conditions and low wind speeds this precondition is not fulfilled anymore and the equations tend to yield unrealistic results. Therefore lower limits for the wind speed and the Obukhov length L are introduced (in order to avoid the so-called intermittency regime that is no longer fully turbulent, see e.g., [29], [30]). The limiting values are set to 0.7 m/s wind speed in 10 m height and $L = -1$ m / +20 m for unstable and stable conditions respectively. In situations with lower wind speeds the vertical profiles of temperature and humidity are determined using these values and the wind speed is set to zero.

3.10. Adaption to varying surface properties

Generally meteorological measurements are performed over open, level terrain with grassland. The accordingly derived profiles are hence only valid for these conditions.

Document downloaded by @DAEL, 2026-11-10 11:56:05 - personal use only

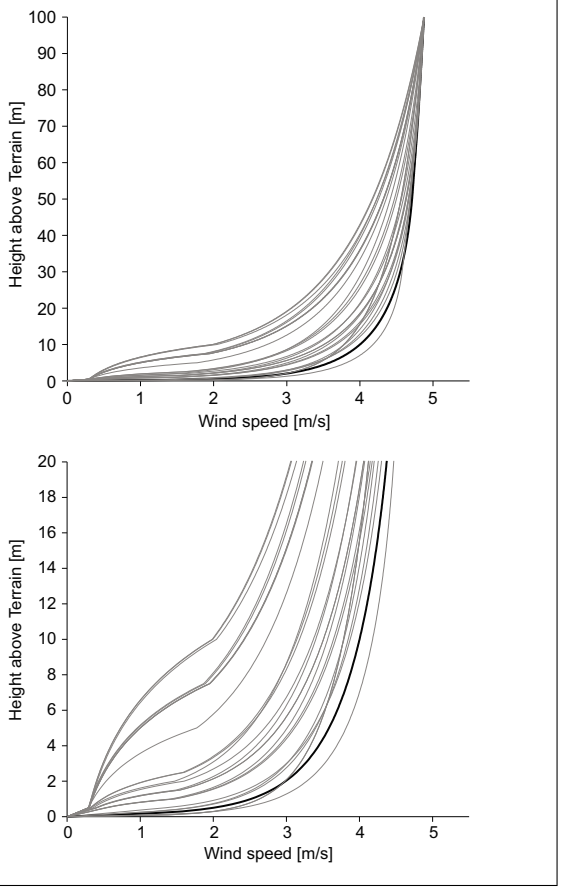


Figure 2. Wind speed profiles for 27 land use types in a situation with a wind speed of 4.9 m/s in 100 m height and a net radiation balance of 50 W/m^2. The profile of the standard surface type for grassland is highlighted. On top the profiles are given up the blending height of 100 m, in the bottom up to 20 m.

In the *sonRAIL* sound propagation model the ground properties can locally change. The ground is not only described by its impedance, which is needed for the calculation of the ground effect, but also by the parameters given under point 3.1. Consequently the profile functions must be adjusted to ground types deviating from the standard conditions. This is done in a way very much like updating the similarity parameters under point 3.6. As a first step the surface radiation balance is recalculated. Then the similarity parameters are adjusted. This time the optimization criteria are not given at the measurement height but at a reference height, generally set to 100 m. The assumption behind this is that wind and temperature become uniform above a certain height (usually called *blending height*, see e.g., [31]) thus reflecting the decreasing local surface influence. The local ground properties are derived for entire Switzerland from a classification scheme of *SwissTopo* that consists of 27 different land use types. Figure 2 gives an example that shows how the ground properties modify the resulting profiles. Mainly on the enlarged view to the right the influence of the roughness sublayer is clearly visible for rough surface types. Note the kink at the roughness sublayer height for the very rough surfaces.

Table I. Classification scheme for weather conditions on the basis of the average wind speed v at a height of 10 m and the net radiation balance Q_*. The representative values for each class are highlighted. (Note: v refers to the magnitude of the wind speed, not the contribution in a certain sound propagation direction.) Unstable: $\geq$ 180 W/m^2 / **250 W/m^2**, Neutral: **50 W/m^2**, Stable: $\leq$-18 W/m^2 / **-25 W/m^2**.

Wind speed v [m/s]		Radiation balance Q_*		
Range	**Average**	Unstable	Neutral	Stable
0–1	**0.0**	U0	N0	S0
1–2	**1.5**	U1	N1	S1
2–3	**2.5**	U2	N2	S2
3–5	**4.0**	U3	N3	S3
>5	**6.0**	U4	N4	S4

4. Statistical analysis procedure

The basis for noise assessments are generally long-term equivalent continuous sound levels L_{eq} (see for example [32]). Calculations that aim at taking meteorological effects into account normally rely on a set of representative meteorological conditions that are calculated individually. The sound exposure levels of each situation are then averaged including a weighting according their frequency of occurrence. The latter is derived by applying a classification scheme on yearly statistics of the local weather conditions. In this section a meteorological classification scheme is presented together with the corresponding standardized profile functions, calculated with the profile generator of section 3.

The classification scheme shown in Table I distinguishes five wind speed classes and three net radiation classes. As the radiation balance is an indication of the associated atmospherical stability, the classes are called *U* for unstable, *N* for neutral and *S* for stable situations. The borders as well as the representative values per class of the net radiation balance are chosen asymmetrically as the effect of changing radiation balance on the resulting temperature stratification is not linear. The classification was set up on the basis of a classification scheme according to Polster [33] with slightly different thresholds (which will be motivated below). The Polster-classes *A* and *B* as well as half of *C* were combined to describe unstable situations and class *G* together with half of class *F* represent stable conditions. The wind speed classes are numbered from 0 to 4 for increasing wind speeds. The class average wind speed in Table I is allocated to a height of 10 m. Additionally a moderate height of roughness elements typical for grassland is employed in the reference profiles.

The corresponding profiles for wind speed and temperature are shown in Figures 3 and 4. The temperature profiles are normalized to zero degree Celsius at a height of 10 m. Both for wind speed as well as temperature the profiles for unstable and neutral conditions are quite similar. This supports the decision taken to reduce the number of radiation balance classes according to Polster for these situations. The resulting temperature gradients under unstable con-

Document downloaded by @DAEL, 2026-11-10 11:56:05 - personal use only

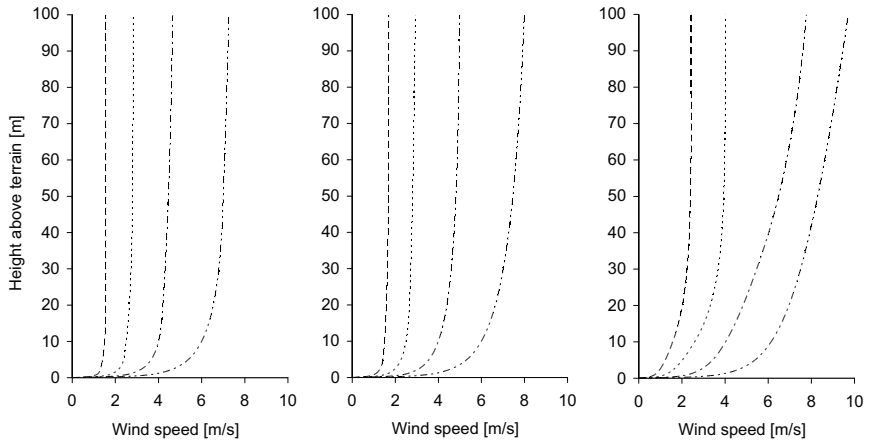


Figure 3. Representative average wind speed profiles are shown for classes U1, N1, S1 (dashed), U2, N2, S2 (dotted), U3, N3, S3 (dash-dotted) and U4, N4, S4 (dash-double dotted). The unstable cases are on the left, the neutral cases in the middle and stable cases on the right. No profile is shown for the classes U0, N0 and S0 as the average wind speed is assumed to be zero.

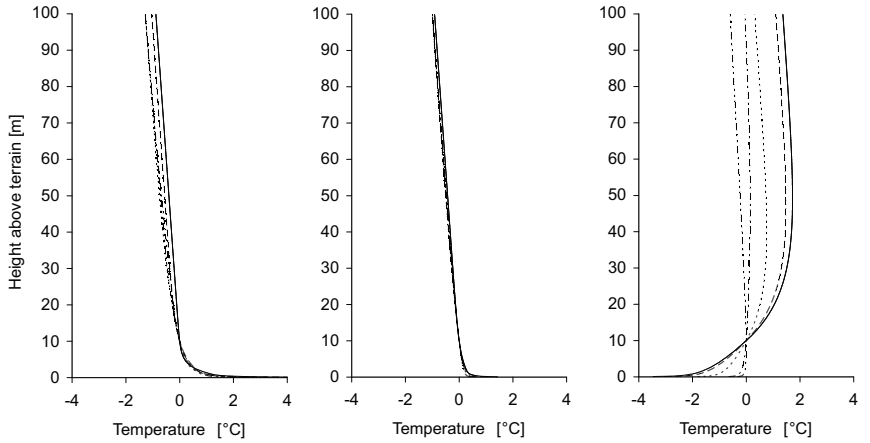


Figure 4. Temperature profiles for the 15 meteorological classes according to Table I, normalized to zero degree Celsius at a height of 10 m. The line style and arrangement of classes corresponds to Figure 3, additionally with classes U0, N0 and S0 as solid lines.

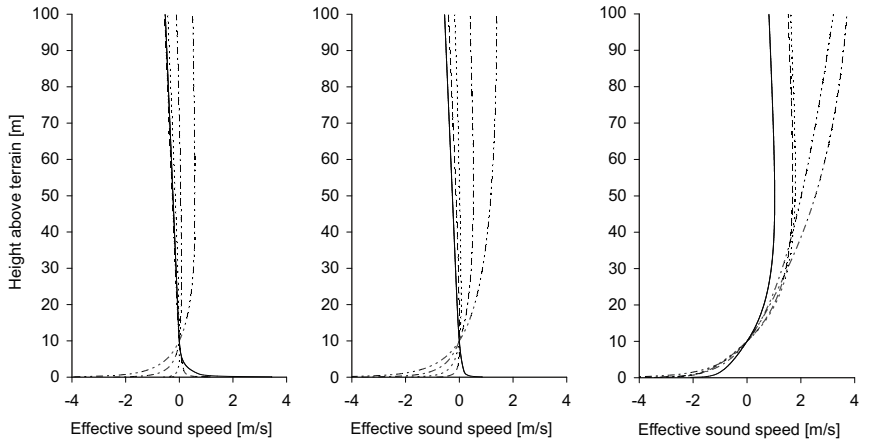


Figure 5. Sound speed profiles under downwind conditions for the 15 meteorological classes according to Table I, normalized to zero m/s at a height of 10 m. The line style and arrangement of classes corresponds to Figure 4.

ditions only deviate significantly from neutral conditions very close to the ground where the unstable cases exhibit major temperature gradients that can not be found under neutral conditions. In contrast the temperature gradients under stable conditions can yield larger values and vary in a more pronounced way in dependence to wind speed even up to the top level. The wind speed profiles under stable conditions also deviate from those under neutral or unstable situations. The wind speed tends to increase significantly up to greater heights, leading to what is described in literature as a low level jet.

Figures 5 and 6 show the resulting sound speed profiles for downwind and upwind conditions. The sound speed profiles of the stable situations in Figure 5 indicate the cumulative effect of wind speed and temperature gradient. Under neutral and unstable conditions the two influences

Document downloaded by @DAEL, 2026-11-10 11:56:05 - personal use only

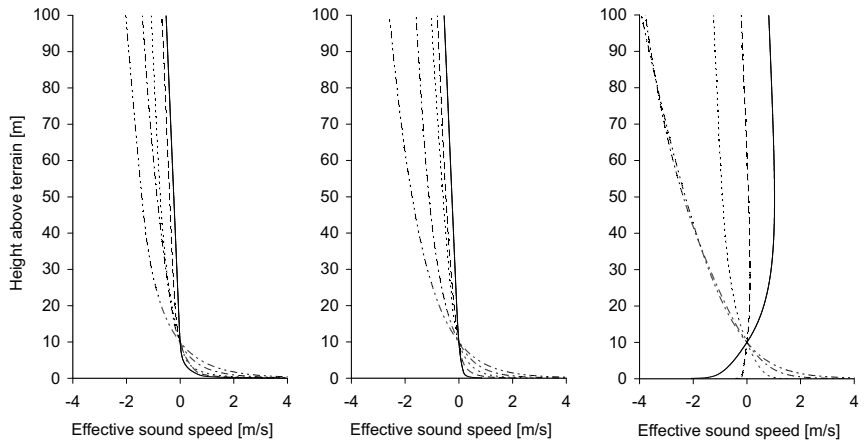


Figure 6. Sound speed profiles under upwind conditions for the 15 meteorological classes according to Table I, normalized to zero m/s at a height of 10 m. The line style and arrangement of classes corresponds to Figure 4.

work in opposite directions. The two influences more or less cancel each other out in the profiles *U2* and *N1*, i.e., at wind speeds of 2–3 and 1–2 m/s, respectively. Hence wind speeds have to be greater than 2 m/s in a neutrally stratified atmosphere or even greater than 3 m/s on a sunny day to clearly overcome the effect of temperature stratification. Under upwind conditions as shown in Figure 6 favorable conditions for sound propagation, i.e. increasing sound speed with height, can only be found in class *S0*, corresponding to nights with a clear sky and wind speeds below 1 m/s.

Especially when looking at Figure 5 it becomes obvious that for unstable and neutral conditions gradients are primarily present in the immediate vicinity of the ground. At greater heights favorable conditions for sound propagation can not be found anymore. Under stable conditions the sound speed profiles are generally more pronounced at greater heights and especially exhibit favorable conditions up to several tens of meters. Consequently it can be deduced that positive meteorological effects on sound propagation, i.e., an increase of sound exposure level, will generally have an impact up to greater distances at night time.

5. Validation results and examples of application

5.1. Comparison of wind and temperature profiles of COSMO-2 with the corresponding standardized profiles

For each horizontal grid point of the COSMO-2 data set a statistical analysis was performed based on the classification scheme presented in section 4. For the present purpose of investigating climatological sound propagation patterns and to avoid local roughness influence, the reference height to produce the wind classes in Table I was set to 100 m above ground. The statistical analyses were then performed for this height. This approach allows to be consistent with the adaption to other surface properties shown in Figure 2, that is performed during the sound propagation calculation.

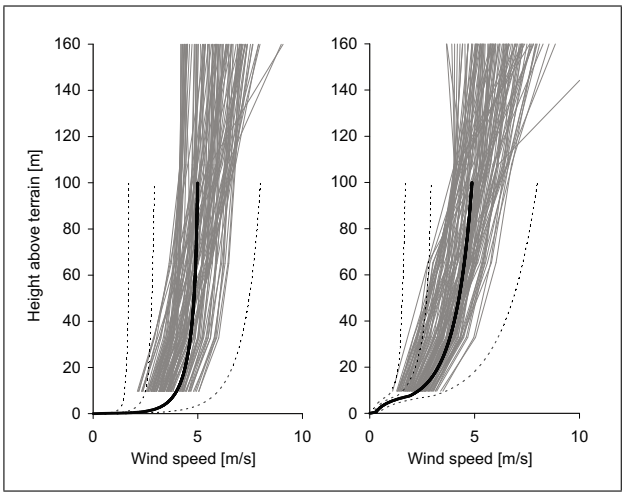


Figure 7. Comparison of wind speed profiles of 100 randomly chosen data sets from a COSMO-2 grid point in grey with the corresponding wind speed profile of the profile generator in black for class *N3* and two grid points with different roughness length z_0. For comparison profiles of the classes *N1*, *N2* and *N4* of the profile generator are depicted as dotted lines. The COSMO-2 data comprises values from the lowest five model surfaces ranging approximately from 10 to 160 m. Attributed to grid point 31'231 (Payerne) to the left is a roughness length z_0 of 0.07 m corresponding to an average height of roughness elements of 0.7 m. The plot on the right shows grid point 17'272 (Wynau) with a roughness length z_0 of 0.88 m.

Figure 7 shows a comparison of two COSMO-2 grid points with 100 data sets each, with the corresponding wind speed profiles of the profile generator for class *N3*, i.e., a situation with only minor temperature gradients but prominent wind. The data sets were taken randomly from the data of the entire year, collected as described in section 2. The two gridpoints were chosen as they are attributed to largely different roughness lengths. The influence of the surface roughness becomes obvious when comparing the resulting wind speeds at the lowest level of COSMO-2, i.e. at a height of approximately 10 meters. As can be seen the accordance of the COSMO-2 data sets

Document downloaded by @DAEL, 2026-11-10 11:56:05 - personal use only

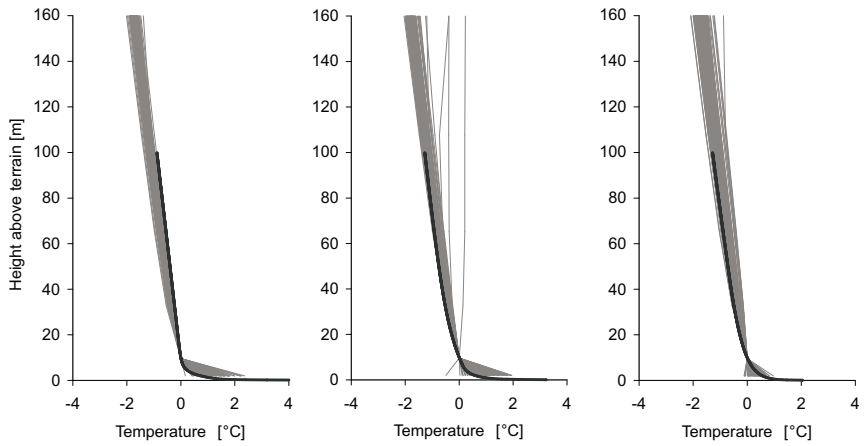


Figure 8. Comparison of temperature profiles of 100 randomly chosen data sets from COSMO-2 grid point 31'231 (Payerne) in grey with the corresponding temperature profiles of the profile generator (thick black line) for classes *U0*, *U2* and *U4*. The COSMO-2 data comprises values from the lowest five model surfaces ranging approximately from 10 to 160 m with an additional value at 2 m.

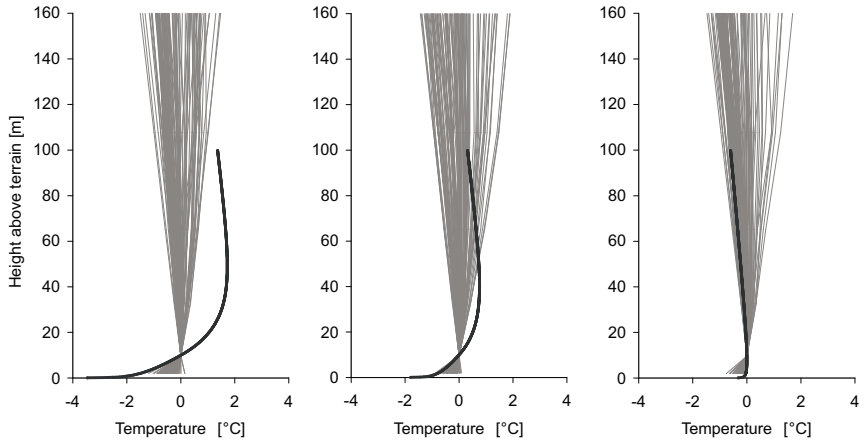


Figure 9. Comparison of temperature profiles of 100 randomly chosen data sets from COSMO-2 grid point 31'231 (Payerne) in grey with the corresponding temperature profiles of the profile generator (thick black line) for classes *S0*, *S2* and *S4*. The COSMO-2 data comprises values from the lowest five model surfaces ranging approximately from 10 to 160 m with an additional value at 2 m.

with the corresponding standardized profiles is fairly good and the effect of differing surface roughness is reproduced correctly. For the other meteorological classes the correspondence is comparable (not shown).

Figures 8 and 9 show temperature profiles for three wind speed classes in conditions with strong incoming or outgoing radiation (unstable and stable cases, respectively). In the unstable cases the temperature profiles are comparably uniform and are represented well by the standardized profiles. Despite the fact that the class width of the radiation balance is much smaller for stable than for unstable situations, the resulting temperature profiles are much more disperse under such conditions. In contrast, the correspondence between the COSMO-2 data set and the present standardized profiles is rather poor for the situations with very weak wind, i.e., in situations with strong nighttime inversions (Figure 9). This is largely due to a breakdown of similarity theory under these conditions – with very low wind turbulence becomes intermittent and there is no corresponding scaling regime, to which the analysis could be changed [29]. Essentially, the turbulence ceases and restarts due to intermittent processes which cannot be treated in the operational COSMO model. Therefore, some minimum turbulence is maintained leading to too small near-surface gradients. The present analysis (i.e., the black curve in Figure 9) similarly assumes similarity theory to hold (but does not assume a minimum exchange) - and thus may be viewed as the limiting behavior for stable low-wind cases.

5.2. Comparison of wind speed distribution with measurement data

With respect to meteorological statistics it is most important to accurately reproduce local wind speed distributions. Therefore the frequency of occurrence of the wind speed classes analyzed with COSMO-2 were compared with data sets collected by conventional stations of the *SwissMetNet* over five years. In Table II the wind speed distributions at four locations in Switzerland are shown. The stations were chosen, on the one hand, to explicitly cover the range of topographical setting. Payerne and Kloten are located in mainly flat terrain, Wynau is in a hilly region and Chur is situated in an alpine valley. On the other hand, they also feature a great variety of roughness lengths z_0 attributed to the associated COSMO-2 grid point.

During daytime the correspondence is fairly good. The COSMO-2 data set only tends to overestimate the frequency of situations with wind speeds above 5 m/s. During nighttime, there is an apparent underestimation of situations with very low wind speed in the model at the ex-

Document downloaded by @DAEL, 2026-11-10 11:56:05 - personal use only

Table II. Probabilities of occurrence of wind velocity classes at four stations, separated into day and night. The first table shows 5-year statistics of *SwissMetNet* stations, the second table shows the corresponding statistics of the COSMO-2 grid points that are closest to the *SwissMetNet* stations and the third Table yields the difference in occurrence between the statistics based on measurements and the COSMO-2 simulations. z_0 refers to the roughness length caused by land-use that is attributed to the associated COSMO-2 grid-points.

SwissMetNet		Day					Night				
Station	z_0	0–1	1–2	2–3	3–5	>5	0–1	1–2	2–3	3–5	> 5
Payerne	0.07	21%	30%	17%	22%	11%	35%	34%	14%	12%	5%
Kloten	0.14	14%	27%	23%	26%	10%	29%	32%	20%	14%	5%
Wynau	0.88	19%	29%	22%	21%	9%	56%	20%	11%	9%	4%
Chur	1.00	10%	16%	15%	32%	26%	33%	24%	18%	18%	8%
COSMO-2		Day					Night				
Station	z_0	0–1	1–2	2–3	3–5	> 5	0–1	1–2	2–3	3–5	> 5
Payerne	0.07	22%	26%	18%	18%	16%	32%	26%	18%	16%	8%
Kloten	0.14	16%	25%	23%	24%	12%	22%	28%	26%	17%	8%
Wynau	0.88	16%	26%	23%	23%	12%	26%	26%	23%	17%	7%
Chur	1.00	8%	13%	16%	34%	30%	17%	21%	30%	25%	7%
Difference		Day					Night				
Station	z_0	0–1	1–2	2–3	3–5	> 5	0–1	1–2	2–3	3–5	> 5
Payerne	0.07	-1%	4%	-1%	4%	-5%	3%	8%	-4%	-4%	-3%
Kloten	0.14	-2%	2%	0%	2%	-2%	7%	5%	-6%	-3%	-3%
Wynau	0.88	3%	3%	-1%	-2%	-3%	30%	-6%	-12%	-8%	-3%
Chur	1.00	2%	3%	-1%	-2%	-4%	16%	3%	-12%	-7%	1%
		1%	**3%**	**-1%**	**0%**	**-4%**	**14%**	**3%**	**-8%**	**-6%**	**-2%**

pense of the 'medium wind speed' classes. This is due to a combination of several factors in the observations and in the model. In quiescent nights the near-surface flow has a tendency to become decoupled from the surface, so that anemometers might come in a 'stop-and-go' mode, in which they need a certain excess speed to get restarted. The model, on the other hand, cannot handle this decoupling and therefore has a tendency to avoid it (by too much mixing).

A comparison of model output and observations always bears the problem that the observation is a point information while the model provides a grid-averaged value ($2.2\times2.2\,\mathrm{km}^2$ in the present case). Under low wind conditions, when the intermittent regime prevails, this is of particular concern and makes a comparison rather difficult.

5.3. Frequency of occurrence of nightly inversions according to COSMO-2-analysis

Figure 10 shows a statistical analysis of the frequency of occurrence of nighttime inversions for Switzerland as an example of the type of analysis that can performed with the present database. The example was chosen as nightly inversions are likely to yield higher sound exposure level and are therefore relevant from an acoustical point of view. As can be seen is the frequency of occurrence exceptionally great in the alpine valleys. Percentages below 45% can only be found in mountainous regions with strong exposition to wind. The average frequency of occurrence around 50% is a convincing explanation why daytime and nighttime long-term averages often systematically deviate.

6. Discussion

The approach presented in this contribution to use meteorological data from a high-resolution NWP model (COSMO-2) instead of measurement data has a number of advantages. The availability of NWP output data at high resolution, good temporal availability and high quality, is a major step forward as such. If the sound propagation modeling had to be based on observations alone, one would have a spatial resolution far from required. Gridded climatological data sets from observations (e.g., [11]) for complex topography as in Switzerland are not available at sufficient resolution and for all variables possibly required. Hence the goal of establishing a 'meteorological data base' that is available for producing sound maps as well as case studies could not be achieved on the basis of observations.

Clearly, the approach has also a number of limiting points:

- The meteorological preprocessor (which is 'borrowed' from air pollution modeling) is based on theory and knowledge from flat horizontally homogeneous terrain. It is clear that wind and temperature profiles will be modified in complex terrain with respect to these ideal profiles - but how exactly is subject of current research (e.g. [34]). However there are indications that at least the surface layer properties are more or less maintained even over relatively complex topography (e.g., [35]).
- Low-wind, stable conditions, which are crucial for sound propagation, are most difficult to handle in both the COSMO model and the profile generator (this is due to the fact that all the theoretical approaches fail

Document downloaded by @DAEL, 2026-11-10 11:56:05 - personal use only

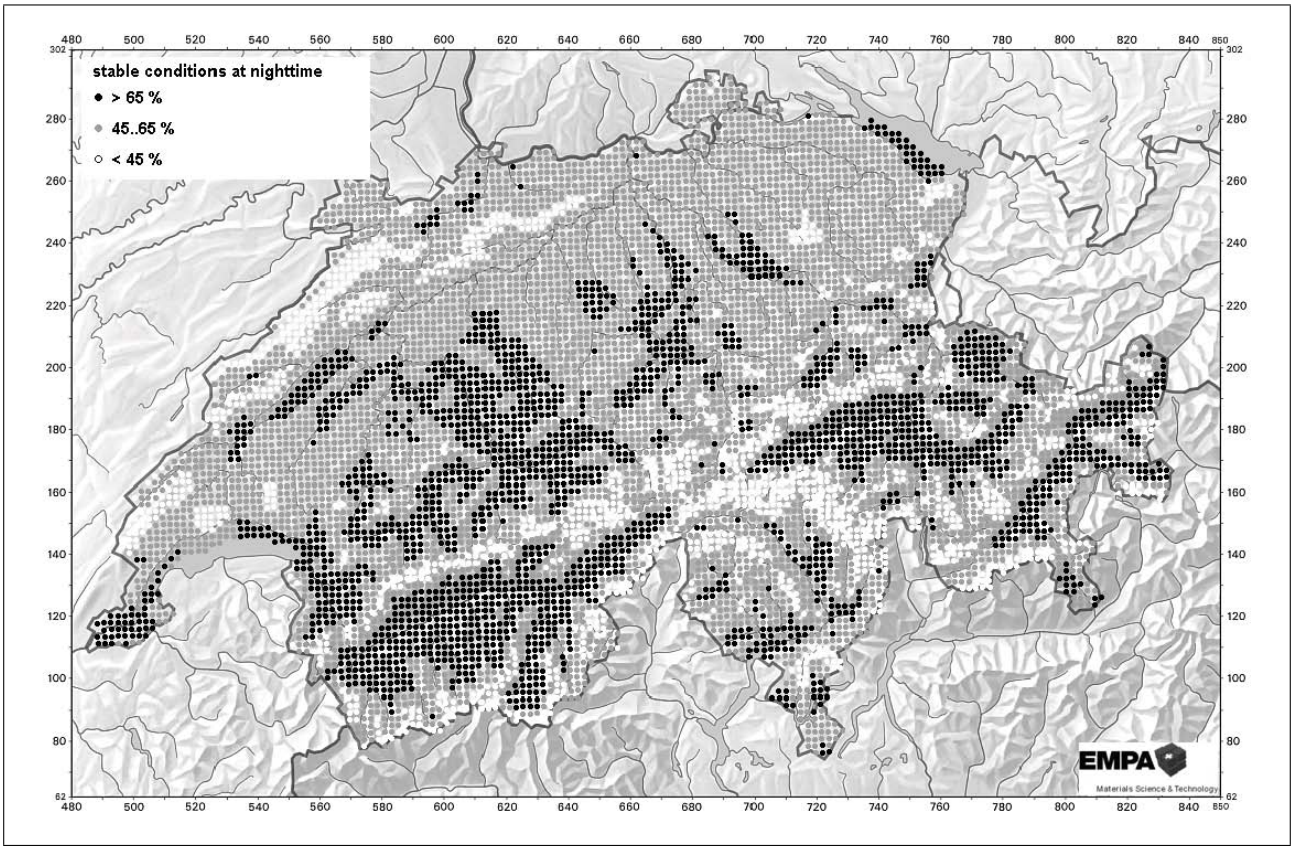


Figure 10. Statistical analysis of the frequency of occurrence of nighttime inversions (classes *S0*, *S1* and *S2*) according to COSMO-2-analysis for Switzerland for the period of March 2008 till the end of February 2009.

for this type of atmospheric condition - and thus simplifying assumptions need to be made - in one way or the other). The present analysis for this meteorological class shows quite distinct differences between COSMO-derived temperature profiles and those based on the profile generator. These differences may be taken as an indication for the uncertainty of the temperature profile under very stable conditions.

- Finally it has to be beard in mind that a spatial resolution of 2 km is still rather coarse for sound propagation modeling. Meteorological effects that take place with a smaller spatial variability than that from the NWP model cannot explicitly be taken into account. For example local wind fields that evolve near waterbodies or at valley slopes are generally not represented. The same applies for wind fields around obstacles. The corresponding profiles would have to be generated in dependence of the wind direction and with a far greater spatial resolution.

Yet, these limitations cannot be overcome with the present meteorological models at hand. Also the profile generator represents the state-of-the-art in the way profiles of wind speed and temperature are calculated. In comparison to other modeling concepts that are used in acoustics many effects are taken into account, that have been neglected so far. For example the introduction of a roughness sublayer or the adaption to varying surface properties is neither included in the work of Salomons, van den Berg et al. [36], [37], that was incorporated in the ISO Standard 13474 [38] nor in the approach of Heimann [7], which was used in the Harmonoise project [39], [40], [41].

The mentioned publications as well as for example the work of Kuehner [42],[43], that is based on the German 'Technische Anleitung zur Reinhaltung der Luft' [44], rely on classification schemes that take wind speed measurements at a height of 10 m and an assessment of the atmospheric stability into account. Typically five to six classes for wind speed as well as atmospheric stability are introduced. For each class representative values of the free parameters of the profile functions are given. For the classification of atmospheric stability different schemes are used, stemming either from Manier [45], Pasquill [46] or Polster [33], which follow the same basic principles and therefore only exhibit minor differences. The atmospheric stability class is thereby generally assigned on the basis of the percentage of cloud cover and a distinction of day and night. This approach to estimate the atmospheric stability class is quite accurate and is especially helpful in the context of the classification scheme proposed in this publication, as it is only based on three atmospheric stability classes.

The decision to use only three stability classes was taken when looking at effective sound speed profiles. Even with widely varying radiation balances the temperature profiles during daytime do not alter significantly. Therefore there is no justification for a representation with several classes. More important are wind speed and direction.

Document downloaded by @DAEL, 2026-11-10 11:56:05 - personal use only

When comparing the wind speed classes it becomes obvious that the classification presented in this publication is more subtle at smaller wind speeds and rougher at greater wind speeds. Heimann as well as ISO 13474 also use five classes in total. Yet the last two classes cover wind speeds of 6 to 10 m/s and greater than 10 m/s. However, according to statistical analysis as for example presented in Table II such high wind speeds are rather unusual and are therefore in the context of long term-averages less important. Apart from the probability of occurrence a narrower classification at smaller wind speeds is also justified as the influence on the temperature stratification is quite considerable. As shown in Figures 5 and 6 the estimation whether a situation is judged as favorable, neutral or unfavorable is highly depending on the wind speed, especially in the range of 1 to 3 m/s.

Acknowledgement

This work was supported by the Federal Office for the Environment of Switzerland (FOEN) and the Defence Procurement Agency of Switzerland (armasuisse).

References

[1] D. van Maercke, J. Defrance: Development of an analytical model for outdoor sound propagation within the harmonoise project. Acta Acustica United with Acustica **93** (2007) 201–212.

[2] J. Kragh, B. Plovsing: Nordic environmental noise prediction method. nord2000 summary report. General nordic sound propagation model an applications in source-related prediction methods. DELTA Acoustics & Vibration Report **1719/01** (2002).

[3] D. Sehu, J. M. Wunderli, K. Heutschi, T. Thron, M. Hecht, A. Rohrbeck, T. Ledermann: sonrail - projektdokumentation. PDF Bundesamt fuer Umwelt (Bafu), 2010. http://www.bafu.admin.ch/laerm/01148/06762/07079 /index.html?lang=de.

[4] R. J. Thompson: Ray theory for an inhomogeneous moving medium. Journal of the Acoustical Society of America **51** (1972) 1675ff.

[5] J. Hofmann, K. Heutschi: An engineering model for sound pressure in shadow zones based on numerical simulations. Acta Acustica United with Acustica **91** (2005) 661–670.

[6] D. Botteldooren: Finite-difference time-domain simulation of low-frequency room acoustic problems. Journal of the Acoustical Society of America **98** (1995) 3302–3308.

[7] D. Heimann, R. Blumrich: Time-domain simulations of sound propagation through screen-induced turbulence. Applied Acoustics **65** (2004) 561–582.

[8] R. Stull: An introduction to boundary layer meteorology. Kluwer Academic Publishers, ISBN 90-277-2769-4 (1994).

[9] U. Hogstrom: Non-dimensional wind and temperature profiles in the atmospheric surface-layer – a re-evaluation. Boundary-Layer Meteorology **42** (1988) 55–78.

[10] P. Kaufmann: Bodennahe regionale Windfelder ueber komplexer Topographie. Ph.D. thesis, ETH Zuerich No. 11565 (1996).

[11] M. Paulat, C. Frei, M. Hagen, H. Wernli: A gridded dataset of hourly precipitation in Germany: Its construction, climatology and application. Met. Zschr. **17** (2008) 719 – 732.

[12] B. Szintai, P. Kaufmann, M. W. Rotach: Simulation of pollutant transport in complex terrain with a NWP - particle dispersion model combination. in press Boundary-Layer Meteorol (2010).

[13] A. Rossa, D. Leuenberger: Sensitivity of the LHN scheme to non-rain echoes. Meteorological Applications **15** (2009) 503–511.

[14] F. Schubiger, P. Kaufmann, C. Hug: Results of the operational verification of meteoswiss. COSMO General Meeting, Offenbach, Germany, 2009.

[15] T. Weusthoff, F. Ament, M. Arpagaus, M. W. Rotach: Assessing the benefits of convection permitting models by neighborhood verification - examples from map d-phase. in press Mon Wea Rev (2010).

[16] C. Hug, P. Kaufmann, D. Ruffieux: Verification of COSMO-2 with independent data from a wind profiler. COSMO Newsletter **10** (2010) 64–69.

[17] P. Mason: The formation of areally-averaged roughness lengths. Quart J Roy Meteorol Soc **114** (2006) 399 – 420.

[18] R. Geiger and others: The climate near the ground. vieweg Textbook Meteorology (1995).

[19] S. R. Hanna, J. C. Chang: Hybrid plume dispersion model (hpdm) improvements and testing at 3 field sites. Atmospheric Environment Part a-General Topics **27** (1993) 1491–1508.

[20] D. Greenland, T. Oke: Boundary-layer climates. Professional Geographer **41** (1989) 388–389.

[21] VDI: Environmental meteorology - interactions between atmosphere and surfaces - calculation of short-wave and long-wave radiation. 1999.

[22] J. A. Businger, J. C. Wyngaard, Y. Izumi, E. F. Bradley: Flux-profile relationships in atmospheric surface layer. Journal of the Atmospheric Sciences **28** (1971) 181–189.

[23] V. Mellert, A. Sill: Meteorologische Einfluesse auf die Schallausbreitung (1986).

[24] M. Sugita, W. Brutsaert: How similar are temperature and humidity profiles in the unstable boundary-layer. Journal of Applied Meteorology **29** (1990) 489–497.

[25] D. Heimann, E. M. Salomons: Testing meteorological classifications for the prediction of long-term average sound levels. Applied Acoustics **65** (2004) 925–950.

[26] D. Heimann, M. Bakermans, J. Defrance, D. Kuhner: Vertical sound speed profiles determined from meteorological measurements near the ground. Acta Acustica United with Acustica **93** (2007) 228–240.

[27] C. Grimmond, T. Oke: Aerodynamic properties of urban areas derived from analysis of surface form. Journal of Applied Meteorology and Climatology **38** (1999) 1262âĂŞ1292.

[28] M. W. Rotach, P. Calanca: Microclimate. in Holton, J. C., Pyle, J. and Curry, J. A. (Eds.), 'Encyclopaedia of Atmospheric Sciences', Academic Press (2002) 1301–1307.

[29] A. A. M. Holtslag, F. T. M. Nieuwstadt: Scaling the atmospheric boundary layer. Boundary-Layer Meteorology **36** (1986) 201 – 209.

[30] S. Gryning: Some aspects of atmospheric dispersion in the stratified atmospheric boundary layer over homogeneous terrain. Boundary Layer Meteorol **90** (1999) 479–494.

[31] E. Bou-Zeid, C. Meneveau, M. Parlange: Large-eddy simulation of neutral atmospheric boundary layer flow over heterogeneous surfaces: Blending height and effective surface roughness. Water Resources Res **40** (2004).

Document downloaded by @DAEL, 2026-11-10 11:56:05 - personal use only

[32] EU: Directive 2002/49/ec of the European Parliament and of the Council of 25 june 2002 relating to the assessment and management of environmental noise. 2002.

[33] G. Polster: Erfahrungen mit Strahlungs-, Temperaturgradient- und Windmessungen als Bestimmungsgroessen der Diffusionskategorien. Meteorologische Rundschau **6** (1969).

[34] M. W. Rotach, D. Zardi: On the boundary layer structure over highly complex terrain: key findings from map. Quarterly J. Roy. Meteorol. Soc. **133** (2007) 937 âĂŞ 948.

[35] M. de Franceschi, D. Zardi, M. Tagliazucca, F. Tampieri: Analysis of second-order moments in surface layer turbulence in an alpine valley. Quart J Roy Meteorol Soc. **135** (2009) 1750 – 1765.

[36] E. Salomons, F. van den Berg, H. Brackenhoff: Long-term average sound transfer through the atmosphere: predictions based on meteorological statistics and numerical computations of sound propagation. 6th international symposium on long range sound propagation, Ottawa (1994).

[37] F. van den Berg, N. Kinneging, E. Salomons: An overview of a method to predict average propagation of shooting noise in order to create computergenerated noise contours arond shooting ranges. internoise 96, Liverpool (1996).

[38] I. O. o. Standardization: Iso 13474: Acoustics - framework for calculating a distribution of sound exposure levels of impulsive sound events for the purposes of environmental noise assessment. 2001.

[39] I. M. Noordhoek, J. D. van der Toorn: Validation of the Harmonoise models. HAR28TR-041109-TNO11.doc **D21** (2005).

[40] J. Defrance, E. Salomons, I. Noordhoek, D. Heimann, B. Plovsing, G. Watts, H. Jonasson, X. T. Zhang, E. Premat, I. Schmich, F. Aballea, M. Baulac, F. de Roo: Outdoor sound propagation reference model developed in the European Harmonoise project. Acta Acustica United with Acustica **93** (2007) 213–227.

[41] D. Heimann: Three-dimensional linearised euler model simulations of sound propagation in idealised urban situations with wind effects. Applied Acoustics **68** (2007) 217–237.

[42] D. Kuehner: Excess attenuation due to meteorological influences and ground impedance. Acustica **84** (1998) 870–883.

[43] D. Kuehner: Schallimmissionsprognose und messung nach der ta laerm. Zeitschrift fuer Laermbekaempfung **46** (1999) 50–60.

[44] Bundesministerium fuer Umwelt, Naturschutz und Reaktorsicherheit: Erste allgemeine Verwaltungsvorschrift zum Bundes-Immissionsschutzgesetz (Technische Anleitung zur Reinhaltung der Luft, TA Luft) (1986).

[45] G. Manier: Ausbreitungsklassen und Temperaturgradienten. Meteorologische Rundschau **28** (1975) 6–11.

[46] J. Seinfeld, S. Pandis: Atmospheric chemistry and physics. New York, 1998.

Document downloaded by @DAEL, 2026-11-10 11:56:05 - personal use only